Supporting Information

Locomotion of Micromotors in Paper Chips

Paula De Dios Andres,[a#] Miguel A. Ramos-Docampo,[a#] Xiaomin Qian,[a] Marian Stingaciu,[b] Brigitte Städler [a]*

[a]Interdisciplinary Nanoscience Center (iNANO), Aarhus University, Gustav Wieds Vej 14, 8000 Aarhus, Denmark

[b]Department of Chemistry, Aarhus University, Langelandsgade 140, 8000 Aarhus C, Denmark

*bstadler@inano.au.dk

[#]These authors contributed equally.

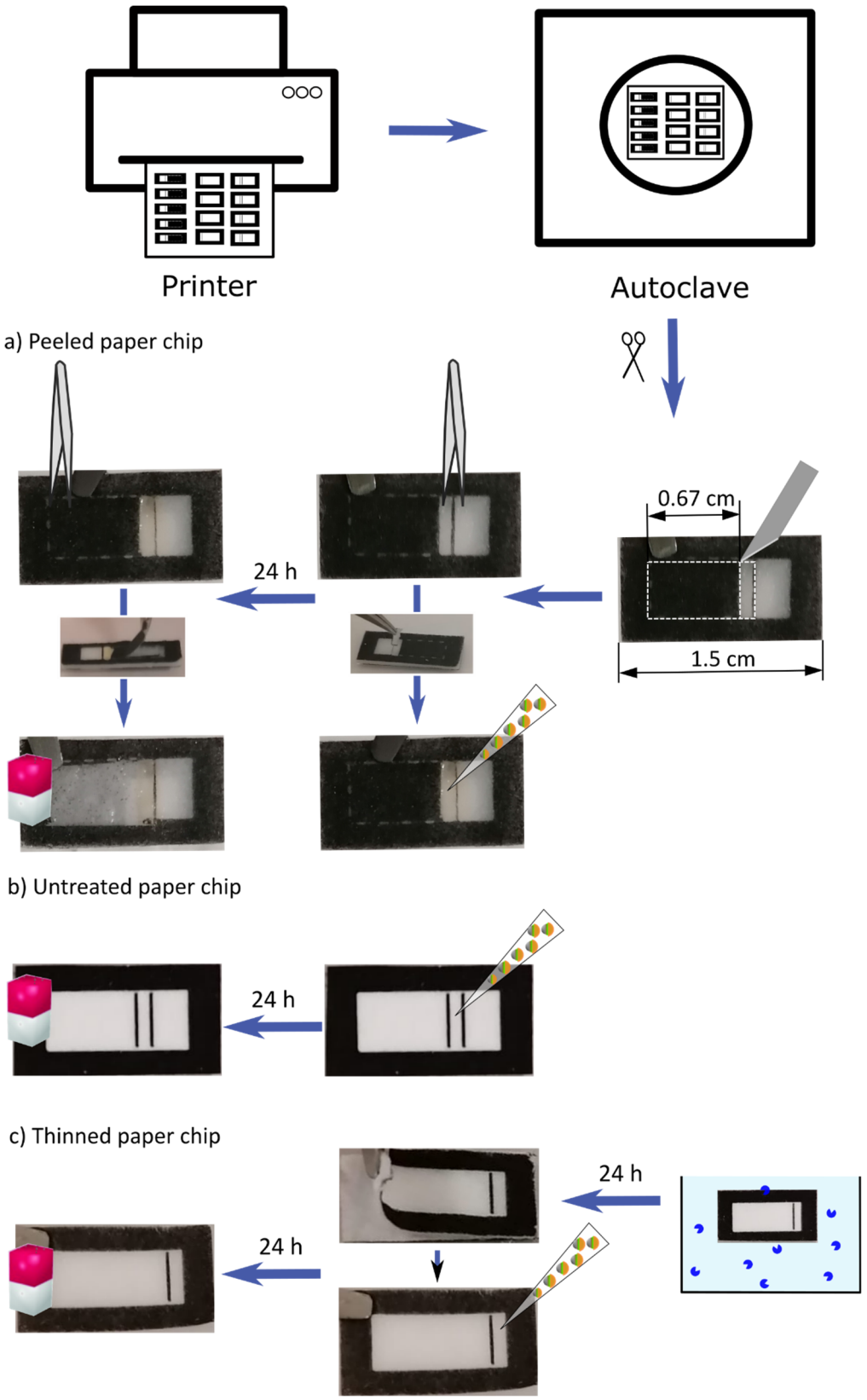

Scheme S1. Schematic of the fabrication process of peeled paper chips (a), untreated paper chips (b), and thinned paper chips (c).

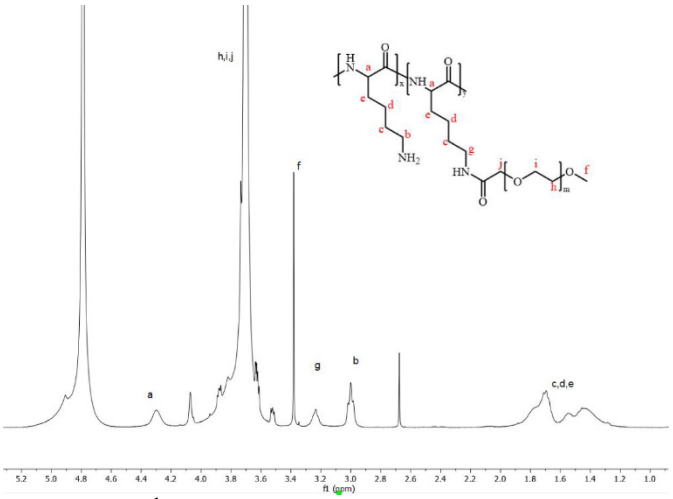

Figure S1. ^{1}H-NMR spectrum of PLL-*g*-PEG in D_2O.

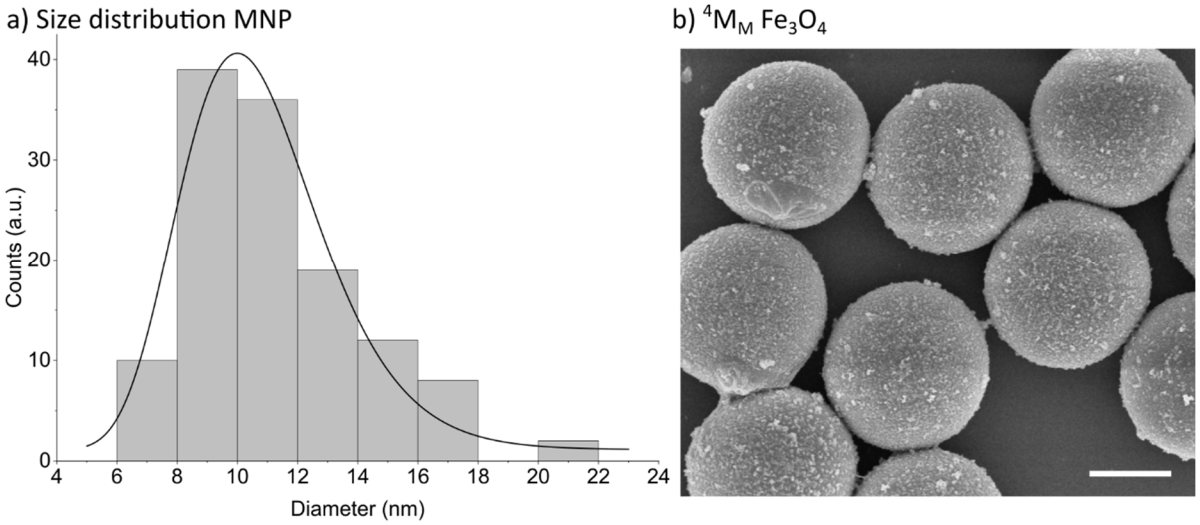

Figure S2. a) Size distribution of MNP determined from TEM images. b) Representative SEM image of the assembly after the MNP deposition onto PAH/PSS pre-coated PS-P (without PSS/PLL terminating layers). Scale bar: 2 μm

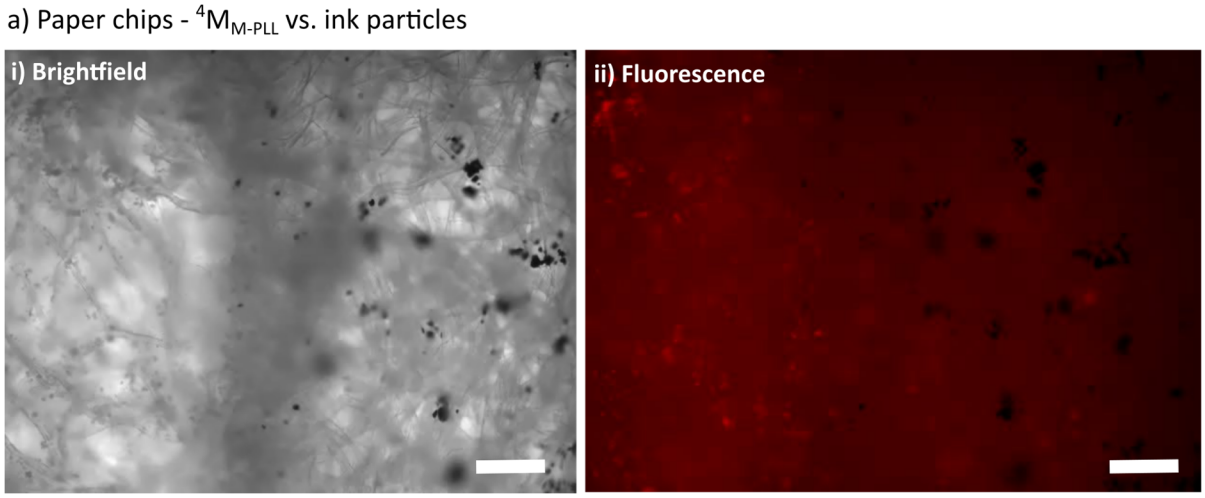

Figure S3. Representative microscopy images of peeled paper chips when $^{4}M_{M\text{-}PLL}$ were added to show the difference between micromotors and ink residues. Images were taken using brightfield (i) or fluorescence (ii). Scale bars: 200 µm.

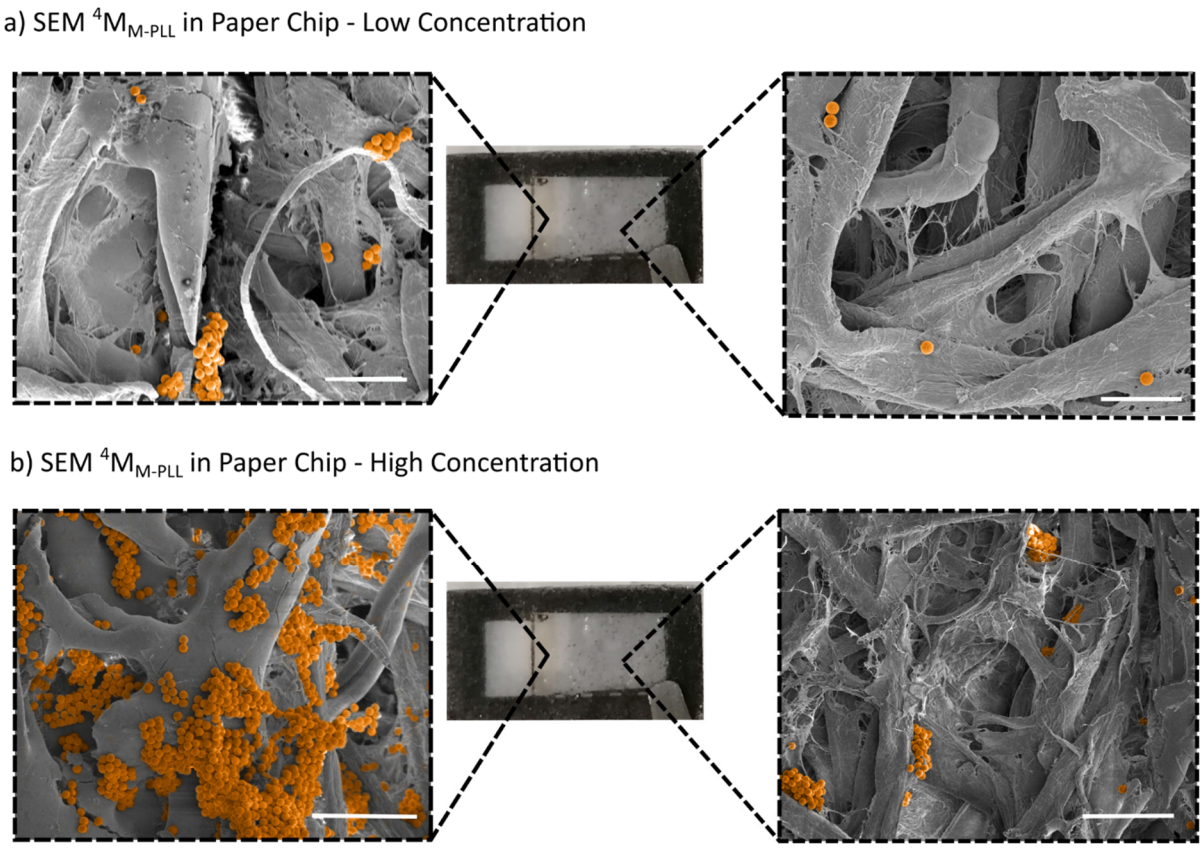

Figure S4. Representative SEM images of peeled paper chips when $^{4}M_{M\text{-}PLL}$ were added at low concentration (a) or ~10× higher density (b). Images were taken in the loading area (left) and at the end of the mobility area (right). $^{4}M_{M\text{-}PLL}$ were artificially colored in orange for better visibility. Scale bars: 100 µm.

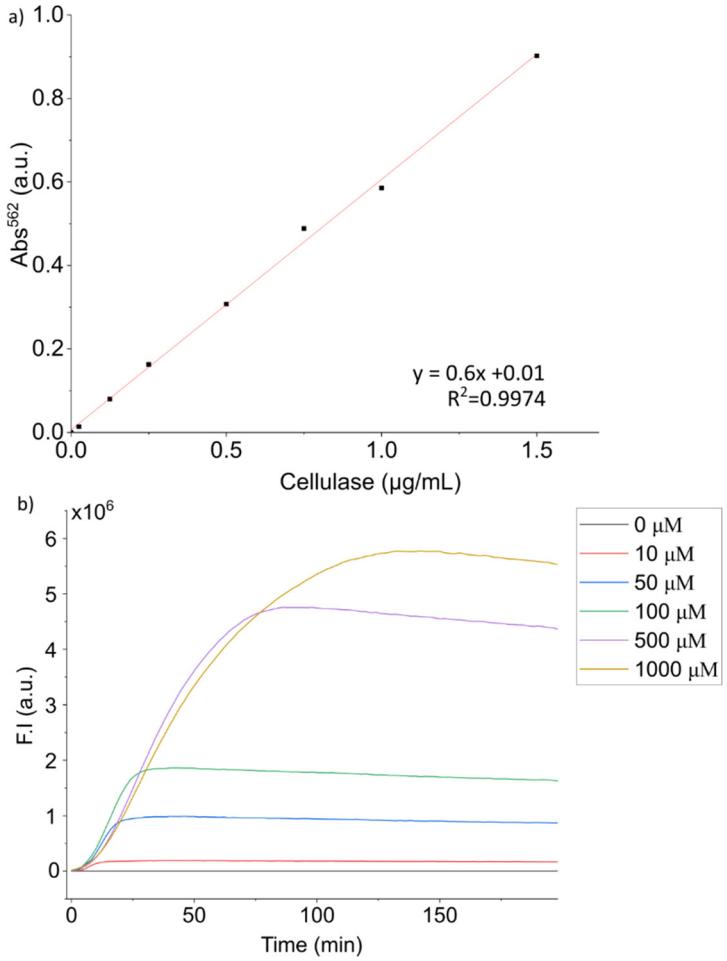

Figure S5. $^{4}M_{M\text{-}C}$ characterization. a) BCA assay of free cellulase used for further assessment of cellulase present on the swimmer surface. b) Activity assay of free cellulase (100 µM) with different substrate concentrations.

First, standard solutions of free cellulase ranging from 25 to 2000 µg mL^{-1} were prepared and used to obtain a calibration curve using the BCA assay by measuring the absorbance at λ = 562 nm. Next, $^{4}M_{M\text{-}C}$ were analyzed using the same assay, and the absorbance value obtained was interpolated in the calibration curve. The cellulase concentration was found to be 0.13 mg mL^{-1}, which corresponded to ~6.5 µg enzyme per mg of PS-P.

The enzyme kinetics obeyed a Michalis-Menten profile obtaining a maximum velocity of 7.66 × 10^{4} mmol s^{-1} and a Michaelis-Menten constant of 52.92 µM. The cellulase activity in $^{4}M_{M\text{-}C}$ was calculated by the following equation:

$$Activity = \left(\frac{C}{\Delta t \times V}\right) \times D$$

where C stands for the concentration of substrate, Δt for the time interval that followed the linear regime of the calibration curve, V of the volume of sample, and D for the dilution factor.

The activity value for the free enzyme was found to be 1.92×10^{-5} U (which was supposed to correspond to 100% of the enzyme activity), while for the $^{4}M_{M\text{-}C}$ was 3.85×10^{-6} U (which translated into a remaining 20% of the activity).

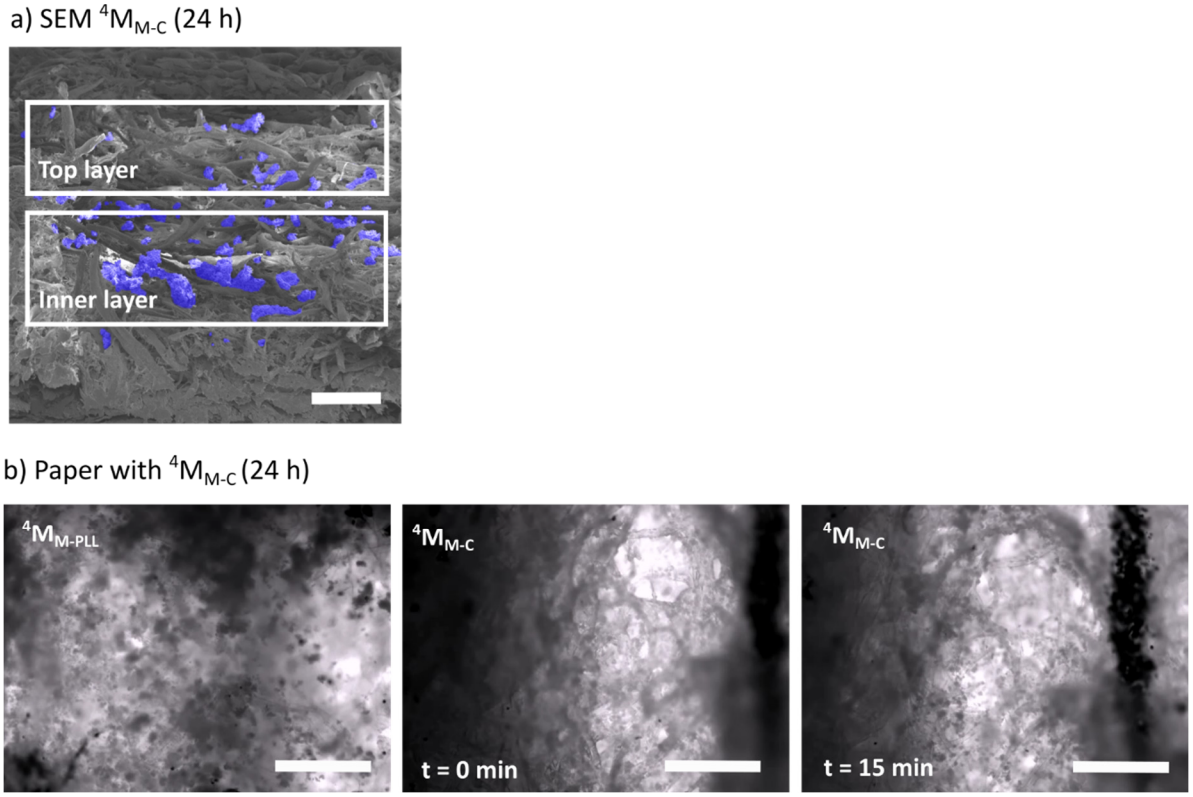

Figure S6. Mobility of $^{4}M_{M\text{-}C}$ after 24 hours. a) Representative SEM image of the cross section of the paper chip after 24 h incubation with $^{4}M_{M\text{-}C}$ (Scale bar: 100 µm). b) Representative microscopy images of different time points of $^{4}M_{M\text{-}C}$ incubated for 24 h compared with $^{4}M_{M\text{-}PLL}$ (Scale bars: 100 µm). $^{4}M_{M\text{-}C}$ were artificially colored in blue for better visibility.

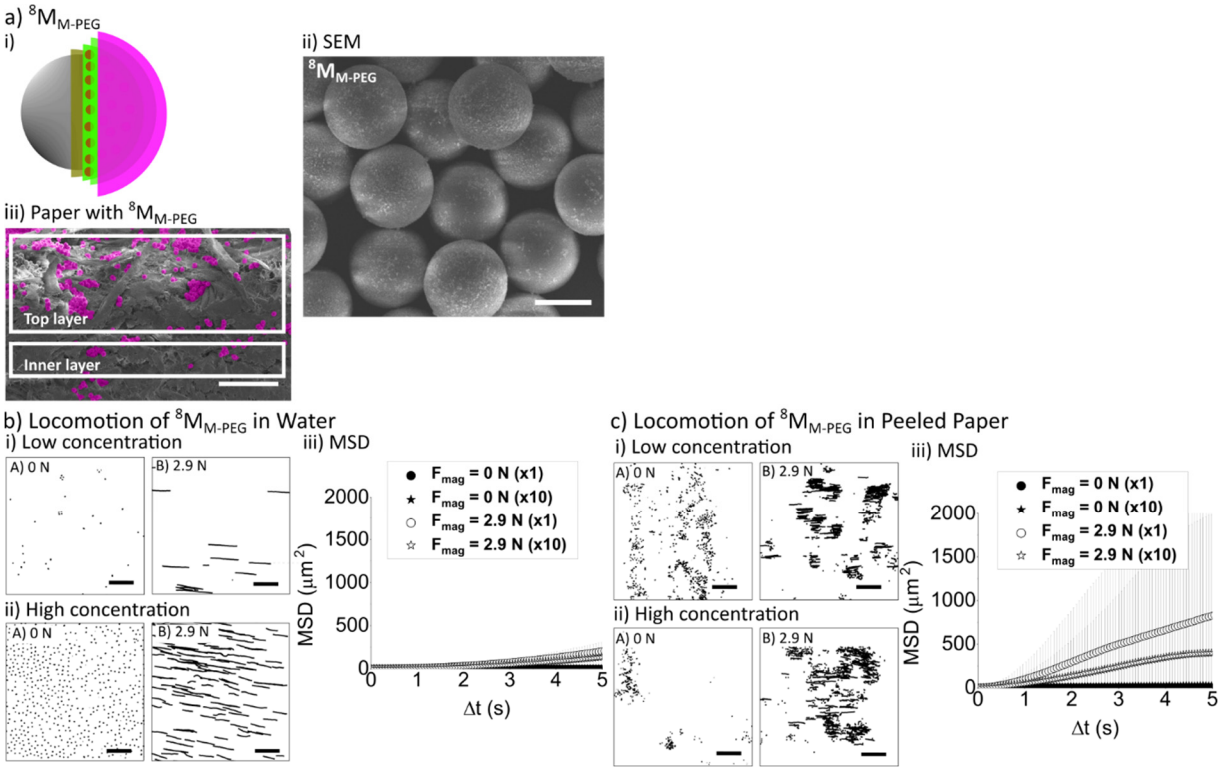

Figure S7. $^{8}M_{M\text{-}PEG}$ mobility in aqueous environment and paper chips. a) i) A cartoon illustrating the different layers in the assembled $^{8}M_{M\text{-}PEG}$ (PS-P: 8 μm PS particle, PSS: poly(sodium 4-styrenesulfonate), PEG: PLL-*g*-PEG). ii) Representative SEM image of the $^{8}M_{M\text{-}PEG}$ (Scale bar: 5 μm). iii) Representative SEM images of the $^{8}M_{M\text{-}PEG}$ distribution in the cross section of the paper chip (Scale bar: 100 μm). $^{8}M_{M\text{-}PEG}$ were artificially colored in purple for better visibility. The locomotion properties of $^{8}M_{M\text{-}PEG}$ in microfluidic channels (b) and peeled paper chips (c). Trajectory maps (i) low concentration; (ii) high concentration and MSD plots (iii) of $^{8}M_{M\text{-}PEG}$ when attracted by 2.9 N magnets. b) Scale bars: 50 μm; c) Scale bars: 250 μm).

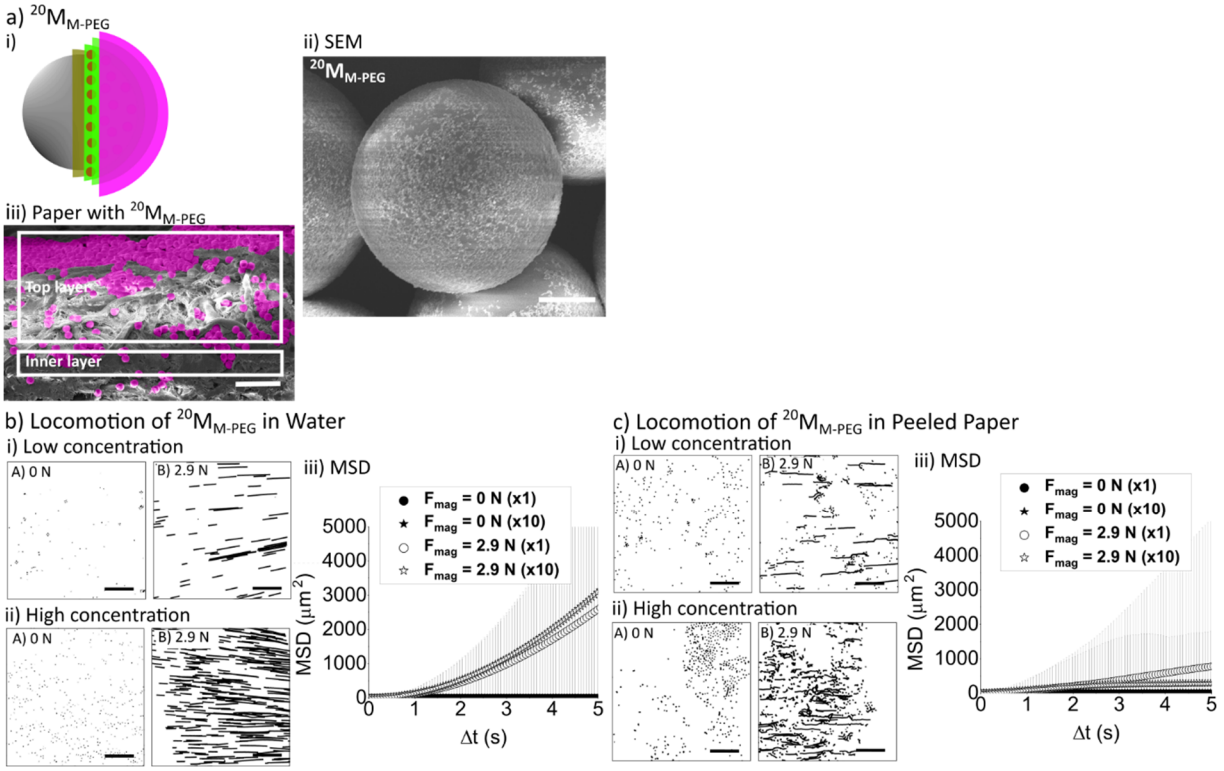

Figure S8. $^{20}M_{M\text{-}PEG}$ mobility in aqueous environment and paper chips. a) i) A cartoon illustrating the different layers in the assembled $^{20}M_{M\text{-}PEG}$ (PS-P: 20 μm PS particle, PSS: poly(sodium 4-styrenesulfonate), PEG: PLL-*g*-PEG). ii) Representative SEM image of the $^{20}M_{M\text{-}PEG}$ (Scale bar: 5 μm). iii) Representative SEM images of the $^{20}M_{M\text{-}PEG}$ distribution in the cross section of the paper chip (Scale bar: 100 μm). $^{20}M_{M\text{-}PEG}$ were artificially colored in purple for better visibility. The locomotion properties of $^{20}M_{M\text{-}PEG}$ in microfluidic channels (b) and peeled paper chips (c). Trajectory maps (i) low concentration; (ii) high concentration and MSD plots (iii) of $^{20}M_{M\text{-}PEG}$ when attracted by 2.9 N magnets. b), c) Scale bars: 250 μm).

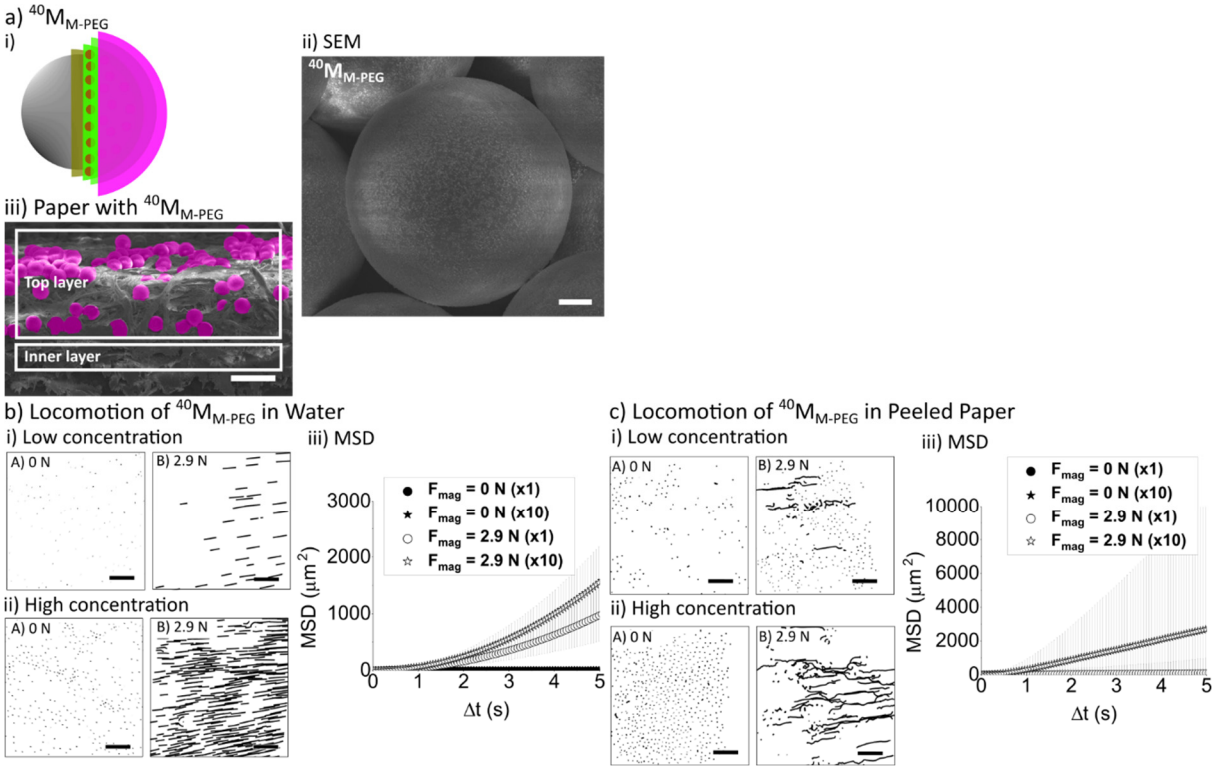

Figure S9. $^{40}M_{M\text{-}PEG}$ mobility in aqueous environment and paper chips. a) i) A cartoon illustrating the different layers in the assembled $^{40}M_{M\text{-}PEG}$ (PS-P: 40 μm PS particle, PSS: poly(sodium 4-styrenesulfonate), PEG: PLL-*g*-PEG). ii) Representative SEM image of the $^{40}M_{M\text{-}PEG}$ (Scale bar: 5 μm). iii) Representative SEM images of the $^{40}M_{M\text{-}PEG}$ distribution in the cross section of the paper chip (Scale bar: 100 μm). $^{40}M_{M\text{-}PEG}$ were artificially colored in purple for better visibility. The locomotion properties of $^{40}M_{M\text{-}PEG}$ in microfluidic channels (b) and peeled paper chips (c). Trajectory maps (i) low concentration; (ii) high concentration and MSD plots (iii) of $^{40}M_{M\text{-}PEG}$ when attracted by 2.9 N magnets. b), c) Scale bars: 250 μm).

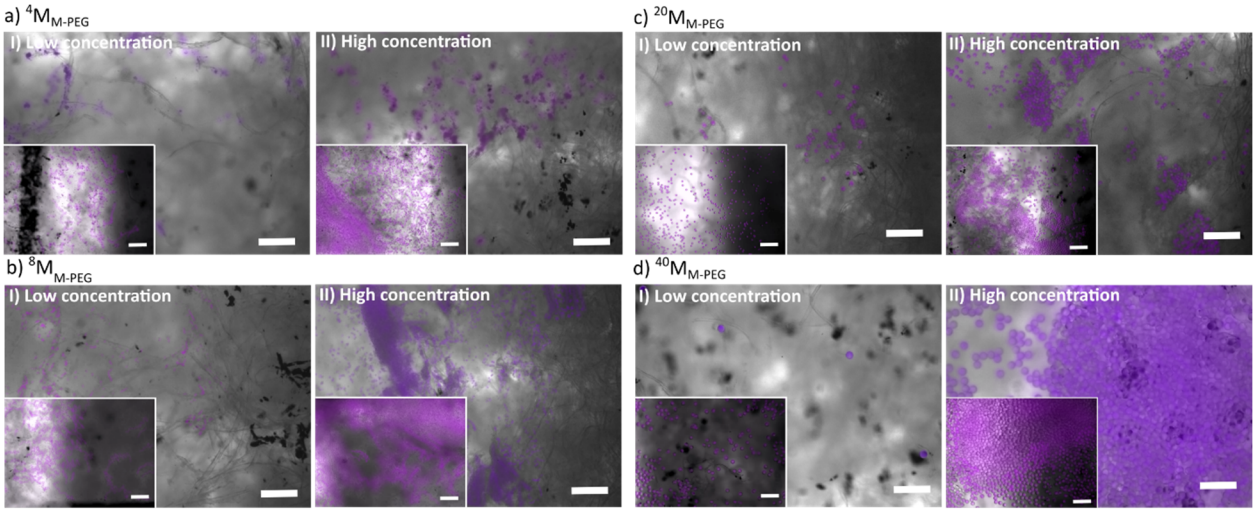

Figure S10. Traveling distance of $^{x}M_{M\text{-}PEG}$: Representative microscopy images of $^{x}M_{M\text{-}PEG}$ at low concentration (I) and high concentration (II) after they moved in peeled paper for ~3 min. The insets in the left corner correspond to the initial amount of micromotors prior to exposure to the magnet (Scale bar: 200 µm). $^{x}M_{M\text{-}PEG}$ were artificially colored in purple for better visibility.

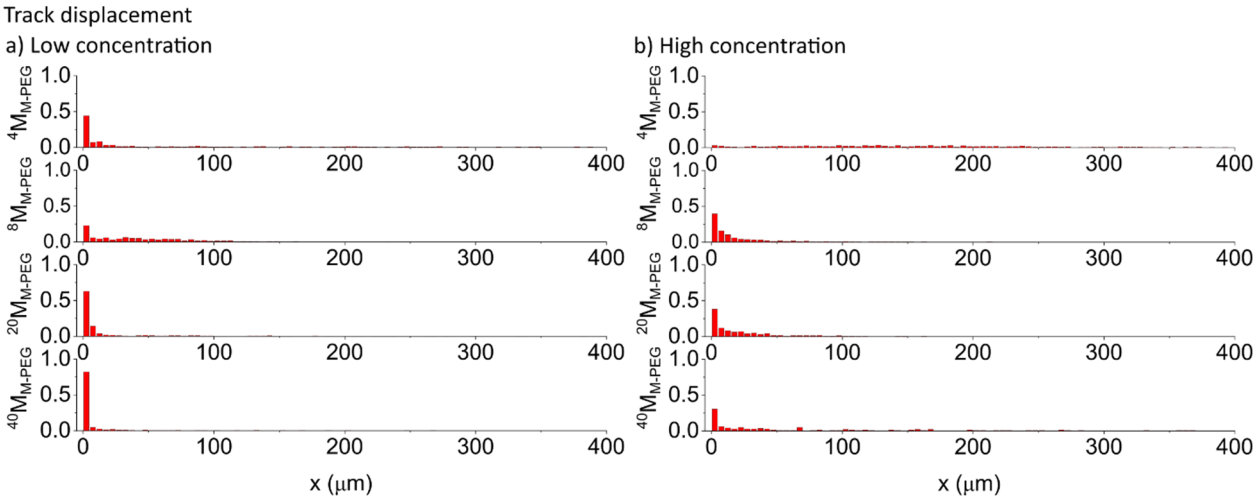

Figure S11. Normalized track displacements of $^{4}M_{M\text{-}PEG}$, $^{8}M_{M\text{-}PEG}$, $^{20}M_{M\text{-}PEG}$, and $^{40}M_{M\text{-}PEG}$ at low and high concentrations in peeled paper chips.

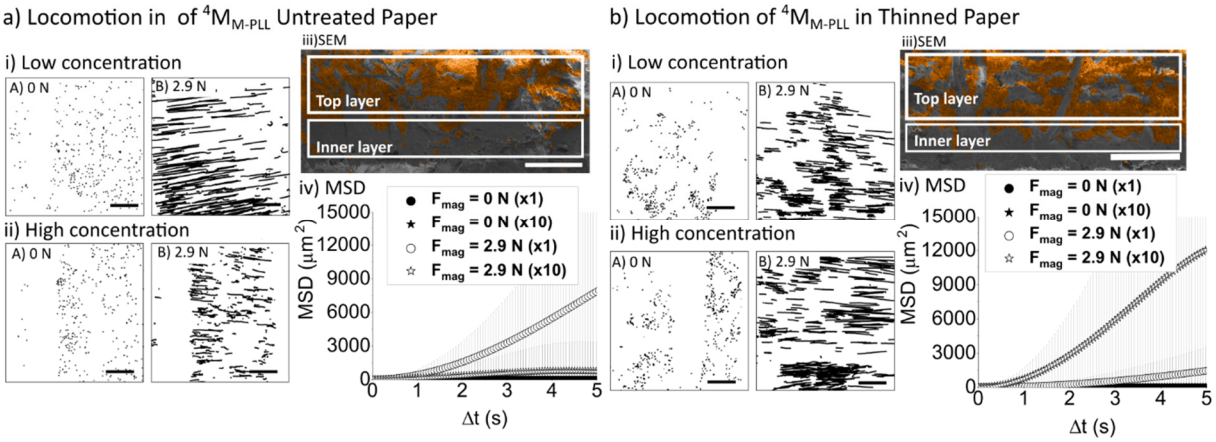

Figure S12. $^4M_{M\text{-}PLL}$ mobility in different environments. a) The locomotion properties of $^4M_{M\text{-}PLL}$ in untreated paper (b) and thinned paper chips (c). Trajectory maps (i) low concentration; (ii) high concentration. iii) Representative SEM images of the $^4M_{M\text{-}PLL}$ distribution in the cross section of the untreated and thinned paper chip (Scale bar: 100 μm). $^4M_{M\text{-}PLL}$ were artificially colored in orange for better visibility. MSD plots (vi) of $^4M_{M\text{-}PLL}$ when attracted by 2.9 N magnets. a), b) Scale bars: 250 μm).

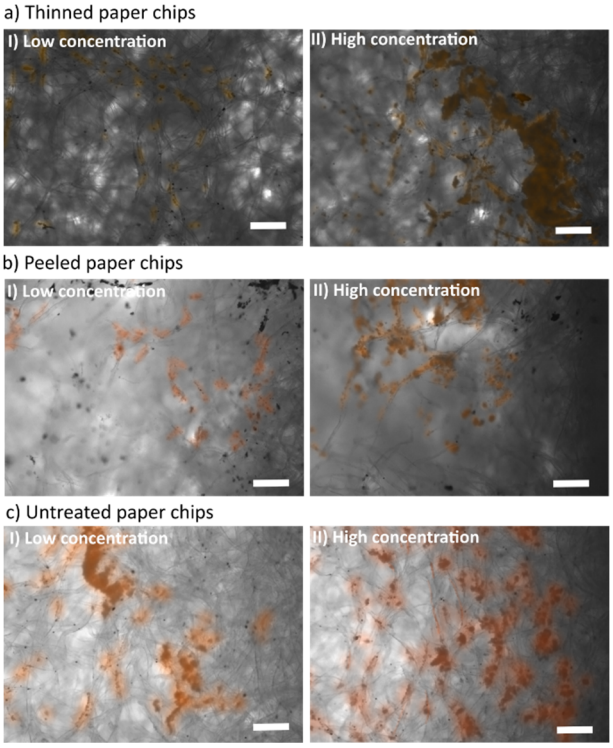

Figure S13. Traveling distance of $^4M_{M\text{-}PLL}$ in different types of paper chips. Representative microscopy images of $^4M_{M\text{-}PLL}$ at low concentration (I) and high concentration (II) after they moved in peeled paper for ~3 min. (Scale bar: 200 μm). $^4M_{M\text{-}PLL}$ were artificially colored in orange for better visibility.

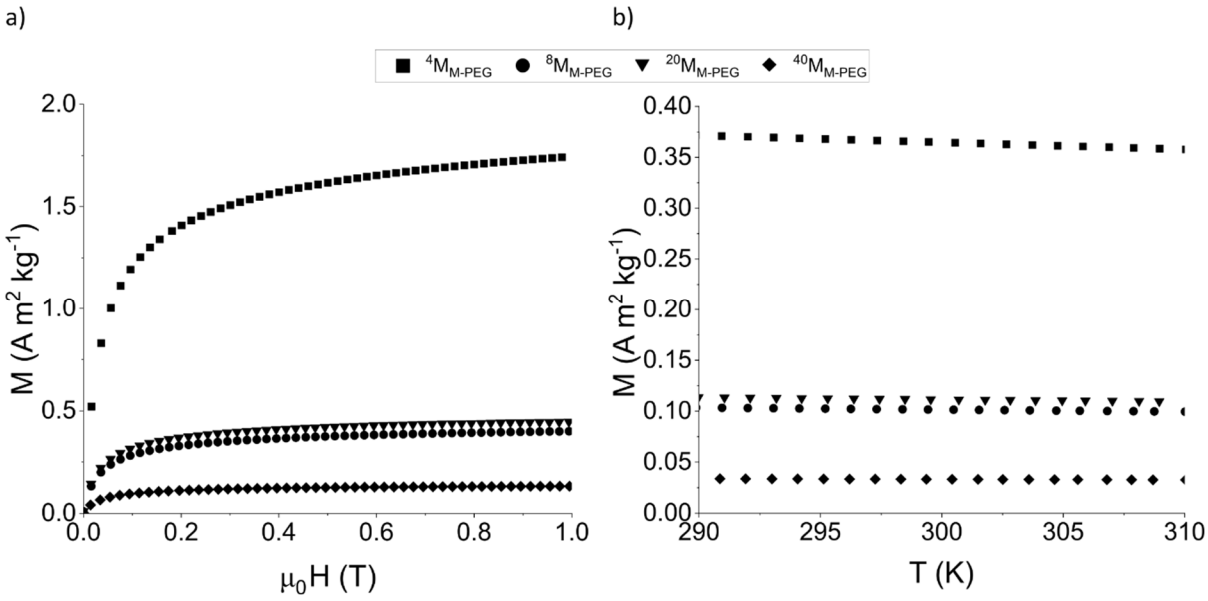

Figure S14. Magnetic measurements of $^{x}M_{M\text{-}PEG}$. a) Virgin curves recorded at 300 K up to a magnetic field of 1 T, and b) magnetization *versus* temperature (M-T) curves recorded at low magnetic field (10 mT).

Table S1. Velocities (v) and interquartile range (in brackets) of $^{4}M_{M\text{-}PLL}$, $^{4}M_{M\text{-}PEG}$, and $^{4}M_{M\text{-}c}$ at low and high concentrations, in water and peeled paper. Note that the interquartile range is defined by IQR = $Q_3 - Q_1$, and contains 50% of the data.

v (µm s^{-1})						
	$^{4}M_{M\text{-}PLL}$		**$^{4}M_{M\text{-}PEG}$**		**$^{4}M_{M\text{-}c}$**	
Conc.	*Low*	*High*	*Low*	*High*	*Low*	*High*
Water	5.00 (0.97)	12.5 (4.51)	6.63 (3.10)	20.8 (9.88)	-	-
Peeled paper	2.66 (6.74)	17.4 (22.0)	25.2 (35.2)	27.6 (32.1)	-	10.9 (11.0)

Table S2. Magnetophoretic mobility (ξ) values of the $^{4}M_{M\text{-}PEG}$, $^{8}M_{M\text{-}PEG}$, $^{20}M_{M\text{-}PEG}$, and $^{40}M_{M\text{-}PEG}$ in water at low concentration, calculated from eqn. 1, considering the viscosity of water at 25 °C (η = 0.89 mPa·s).

	R_P (µm)	**R_H (µm)**	**Δχ**	**ξ (×10^{-23} m^3 T^{-1} A^{-1} s^{-1})**	**ξ/R^2 (m T^{-1} A^{-1} s^{-1})**
$^{4}M_{M\text{-}PEG}$	2	2.39	0.2369	9.88	24.71
$^{8}M_{M\text{-}PEG}$	4	4.85	0.0659	1.09	6.79
$^{20}M_{M\text{-}PEG}$	10	*	0.0724	9.04	9.04

$^{40}M_{M\text{-}PEG}$	20	*	0.0216	1.08	2.70

*Due to the large size of these motors, the hydrodynamic radii could not be measured by DLS, hence the particle radii were considered instead for the calculations.

Table S3. Determination of the colored areas to estimate the percentage of $^{x}M_{M\text{-}PEG}$ that traveled from the loading area to the magnet proximity (~0.67 cm) in 3 min.

	$^{4}M_{M\text{-}PEG}$		**$^{8}M_{M\text{-}PEG}$**		**$^{20}M_{M\text{-}PEG}$**		**$^{40}M_{M\text{-}PEG}$**	
Conc.	*Low*	*High*	*Low*	*High*	*Low*	*High*	*Low*	*High*
Colored Area (%)	4.87	7.32	6.65	30.22	1.91	12.59	0.57	71.98
$^{x}M_{M\text{-}PEG}$ that reached the end of the paper (%)	13	31	27	38	17	36	7	45

Table S4. Determination of colored area used to estimate the number of $^{4}M_{M\text{-}PLL}$ that traveled from the loading area to the magnet proximity (~0.67 cm) in 3 min in the different paper environments.

	Thinned paper		**Peeled paper**		**Untreated paper**	
Conc.	*Low*	*High*	*Low*	*High*	*Low*	*High*
% Colored Area	6.57	20.45	3.66	13.93	26.90	28.76
Number of $^{4}M_{M\text{-}PLL}$	9569	29801	5334	20294	19492	20839